

doi:10.15199/48.2018.02.09

Lightning currents and overvoltages in underground radiating cables of intrusion detection system

Abstract. The paper presents an analysis of exposure of intrusion detection system with underground radiating cable sensors to a threat caused by lightning strike. The peak values of lightning currents and overvoltages in the system components are calculated using a simplified circuit model and PSpice simulation. The results are verified by comparison to the results of a semi-analytical calculation based on a transmission-line model. Various network configurations of the intrusion detection system as well as different grounding conditions are analyzed.

Streszczenie. W pracy przedstawiono analizę narażenia udarowego w systemie ochrony obwodowej z podziemnymi kablami sensorycznymi, powodowane wyładowaniem piorunowym. Do obliczeń rozptyłu prądu pioruna i przepięć w elementach systemu zastosowano uproszczony model obwodowy. Wyniki zweryfikowano wykorzystując model linii transmisyjnej. Analizowano różne konfiguracje oraz różne warunki uziemienia systemu ochrony obwodowej. (Prądy piorunowe i przepięcia w podziemnych kablach sensorycznych systemu ochrony obwodowej).

Keywords: lightning currents; lightning overvoltages; underground sensor cables; intrusion detection system.

Słowa kluczowe: prądy piorunowe; przepięcia atmosferyczne; podziemne kable sensoryczne; system ochrony obwodowej.

Introduction

Lightning is a serious source of damage or interference to electrical and electronic circuits, equipment and systems. Particularly endangered are those systems, which include large outdoor components due to their exposure to direct lightning strikes and to lightning electromagnetic fields. In order to protect electrical and electronic systems against direct strikes, adequate Lightning Protection System (LPS) shall be used [1]-[2]. However, long cable systems spread over large areas are usually not protected by LPS due to economic reasons. An intrusion detection system based on underground radiating cable sensors is the subject of this paper. Typical lightning threats include direct strikes to overhead components and metallic structures or to the earth close to the underground system. It is very likely that some part of lightning current can penetrate the system. That part of lightning current or the lightning-induced current can cause overvoltages and lead to interference or damage.

The intrusion detection system is composed mainly of electronic controllers, coaxial radiating cable sensors of several hundred meters in length, and cable terminators [3]. The system components are buried in the ground at a depth of 23 cm to 40 cm. Each controller is locally grounded, with the required grounding resistance not exceeding the typical value of 10 Ω . The system can be realized as standalone, with a single controller and sensor cables usually routed along an open line, or as a network, with many controllers and sensor cables forming an open line or a closed loop. Electrical power can be supplied to each controller by additional wires or through the sensor cables. In the latter case only one or some controllers are directly connected to the power mains.

Analysis of such systems is rarely met in the literature [4]. Rare are also studies on lightning effects in overhead and underground systems using analytical calculations. Such problems are usually solved numerically [5]-[6]. The analytical formulation for single cables was published by Vance in [7]. However, this is difficult to adopt for fast engineering calculations. The aim of the analysis presented here is to give a simplified technique for estimation of maximum values of surge currents and voltages arising at the system components due to penetration of a part of lightning current into the system in its typical configurations. This information is needed by engineers to assess the threat related to various effects of lightning currents and to electrical breakdown of the system components as well as

to compare the level of threat for different configurations of the system. The results of simplified calculations are compared to those obtained using the transmission-line (TL) model adopted in [8]. Very simple circuit models applying PSpice [9] for simulations are also considered here. This work develops the research presented in [10].

Configurations of intrusion detection system

A single sensor for detecting intrusion is composed of two coaxial cables, up to 400 m in length, called radiating cables: a transmitter and a receiver. These cables run in parallel, 1.5 m distance apart, and are connected to the same controller. In network configurations, each controller in the system typically handles two pairs of such cables. The terminators of cables associated with one controller are usually directly connected to the terminators of cables belonging to neighboring controllers, so that galvanic continuity between the system components is kept [3].

The analysis is focused on the following typical configurations of the system:

- Conf. 1: two controllers, each handling one cable sensor forming a straight open line (Fig. 1a).
- Conf. 2: three controllers, handling one or two cable sensors forming a straight open line (Fig. 1b).
- Conf. 3: six controllers, each handling two cable sensors forming a regular hexagon loop (Fig. 1c).

Assume that a part of lightning current penetrates the metallic enclosure of controller C1 (Figs. 1a-c) and the insulation of the system withstands the threat. Hence, the surge current flows through the outer conductors of the sensor cables and is partially dissipated to the ground by local earthing electrodes of the controllers. The contribution of the inner conductors of the cables to the current flow is neglected [7]. Potentials of grounding electrodes may be considered as approximate measures of threat of electrical breakdown to the components of the system.

Simple-circuit (SC) models

The electrical scheme of the simple-circuit (SC) model for Configuration 1 (Fig. 1a) is shown in Fig. 2a, where R_e and L_e denote respectively the equivalent resistance and inductance of the outer conductor of the base cable section. The scheme from Fig. 2a is represented to its equivalent as shown in Fig. 2b. No additional elements are provided for modeling of the controllers and cable terminators.

Equivalent resistance R_e and inductance L_e of the sensor cable (Fig. 2) have been calculated using formulas [7]:

$$(1) \quad R_e = \frac{l}{\sigma_{Cu} \pi (r_2^2 - r_1^2)}$$

$$(2) \quad L_e = \frac{\mu_0 l}{2\pi} \ln \frac{b}{a}$$

where: l – length of the sensor cable (m); σ_{Cu} – conductivity of the copper conductor (S/m); r_1 and r_2 – inner and outer radius of the cable outer conductor (m); a and b – inner and outer radius of the cable external insulation (m); $a = r_2$ (see Fig. 4); μ_0 – magnetic permeability of the media (H/m).

Note that formula (1) is valid for DC and (2) presents the external inductance of the cable. The conductor internal inductance may be neglected. Assumptions adopted in [10] were different.

Typical parameters of the sensor cable of intrusion detection system [11] and the calculated resistance and inductance of the cable outer conductor are shown in Table 1.

Table 1. Parameters of sensor cables

Parameter	Unit	Value
Conductivity of the outer conductor (copper foil)	S/m	$58.6 \cdot 10^6$
Inner radius of the outer conductor	mm	6.035
Outer radius of the outer conductor	mm	6.365
Inner radius of the cable insulation	mm	6.365
Outer radius of the cable insulation	mm	7.75
Equivalent resistance R_e of the cable ($l=400$ m)	Ω	0.53
Equivalent inductance L_e of the cable ($l=400$ m)	μH	15.75

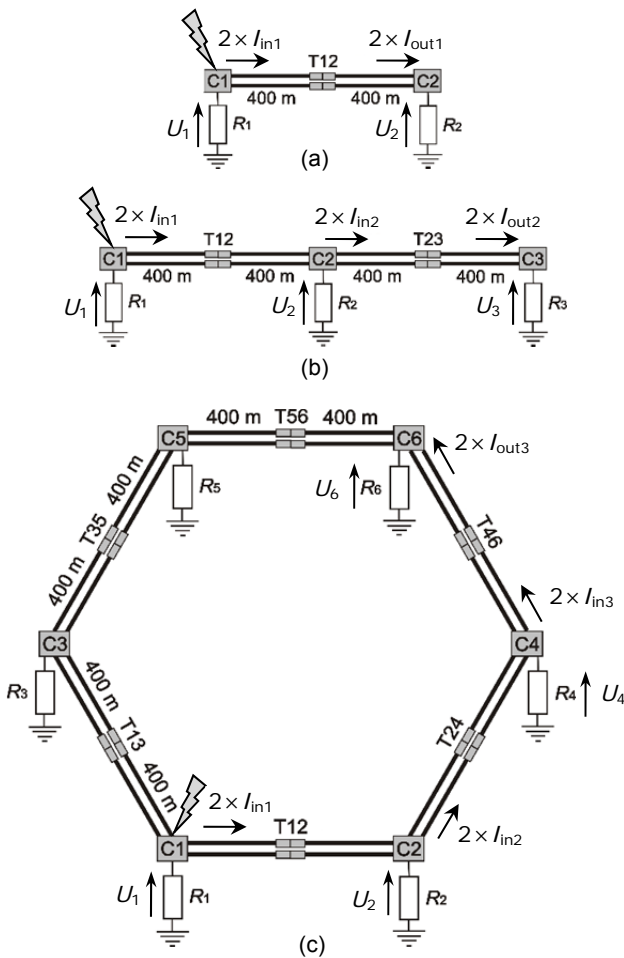


Fig. 1. Configurations of the intrusion detection system: Conf. 1 (a), Conf. 2 (b), Conf. 3 (c). Presented symbols of currents and voltages are used in Tables 2-3 and in Figs. 6-10. Other symbols:

- C1, ..., C6 – controllers;
- Tij – cable terminators;
- R_1, \dots, R_6 – grounding resistances.

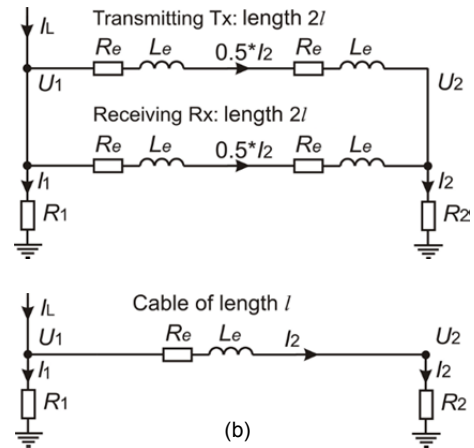


Fig. 2. Equivalent schemes of Conf. 1 (Fig. 1a): simple circuit (SC) model (a) and its equivalent (b) [10];

- I_L – lightning current;
- R_e – equivalent resistance of the base section l of the cable;
- L_e – equivalent inductance of the base section l of the cable;
- R_1, R_2 – local grounding resistances of the controllers.

Deriving the simplified formulas presented here we have assumed that the front steepness of the lightning current dI_L/dt is constant in time. Therefore, factors A, B , and C in formulas (3)-(21) are constant.

According to the equivalent scheme shown in Fig. 2b, the peak values of currents I_1, I_2 have been calculated using the following formulas:

$$(3) \quad I_1 = A \cdot I_L$$

$$(4) \quad I_2 = (1 - A) \cdot I_L$$

where: A – factor describing the current distribution.

Basing on equivalent scheme presented in Fig. 2b, one can obtain the input equation:

$$(5) \quad (R_2 + R_e) \cdot I_2 + L_e \cdot \frac{dI_2}{dt} = R_1 \cdot I_1$$

Substituting (4) into (5) and transforming the formula, we calculate factor A :

$$(6) \quad A = \frac{(R_2 + R_e) \cdot I_L + L_e \cdot \frac{dI_L}{dt}}{(R_1 + R_2 + R_e) \cdot I_L + L_e \cdot \frac{dI_L}{dt}}$$

The equivalent circuits for Conf. 2 and Conf. 3 (Figs. 1b and 1c, respectively) have been created analogously. They are shown in Fig. 3.

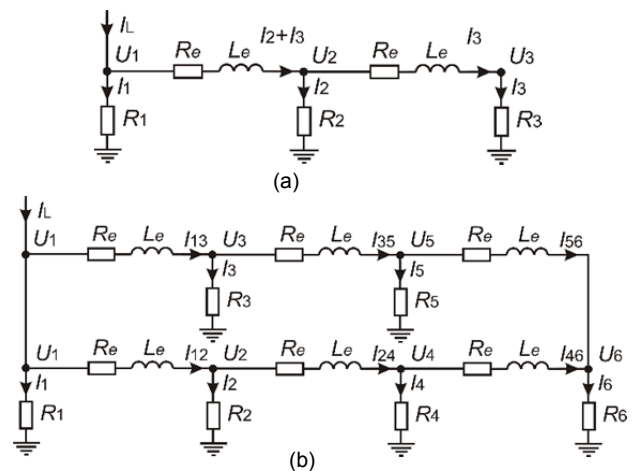


Fig. 3. Equivalent SC schemes for Conf. 2 (a) and Conf. 3 (b)

The formulas for calculation of currents and voltages for Configuration 2 (Fig. 3a) are as follows:

$$(7) \quad I_1 = A \cdot I_L$$

$$(8) \quad I_2 = B \cdot I_L$$

$$(9) \quad I_3 = (1 - A - B) \cdot I_L$$

$$(10) \quad \begin{cases} (R_3 + R_e) \cdot I_3 + L_e \cdot \frac{dI_3}{dt} = R_2 \cdot I_2 \\ R_2 \cdot I_2 + R_e \cdot (I_2 + I_3) + L_e \cdot \frac{d(I_2 + I_3)}{dt} = R_1 \cdot I_1 \end{cases}$$

$$(11) \quad A = \frac{(R_3 + R_e) \cdot I_L + L_e \cdot \frac{dI_L}{dt} + \frac{1}{R_2 \cdot I_L} \cdot \left(R_e \cdot I_L + L_e \cdot \frac{dI_L}{dt} \right) \cdot \left[(R_2 + R_3 + R_e) \cdot I_L + L_e \cdot \frac{dI_L}{dt} \right]}{(R_3 + R_e) \cdot I_L + L_e \cdot \frac{dI_L}{dt} + \frac{1}{R_2 \cdot I_L} \cdot \left[(R_1 + R_e) \cdot I_L + L_e \cdot \frac{dI_L}{dt} \right] \cdot \left[(R_2 + R_3 + R_e) \cdot I_L + L_e \cdot \frac{dI_L}{dt} \right]}$$

$$(12) \quad B = A \cdot \frac{1}{R_2 \cdot I_L} \cdot \left[(R_1 + R_e) \cdot I_L + L_e \cdot \frac{dI_L}{dt} \right] - \frac{1}{R_2 \cdot I_L} \cdot \left(R_e \cdot I_L + L_e \cdot \frac{dI_L}{dt} \right)$$

where: I_1, I_2, I_3 – currents flowing into grounding electrodes of controllers.

Assuming that $R = R_1 = R_2 = R_3 = R_4 = R_5 = R_6$, the formulas for Conf. 3 (Fig. 3b) are as follows:

$$(13) \quad I_1 = A \cdot I_L$$

$$(14) \quad I_2 = I_3 = B \cdot I_L$$

$$(15) \quad I_4 = I_5 = C \cdot I_L$$

$$(16) \quad I_6 = (1 - A - 2 \cdot B - 2 \cdot C) \cdot I_L$$

$$(17) \quad I_{46} = I_{56} = \frac{1}{2} \cdot I_6$$

$$(18) \quad I_{24} = I_{35} = \frac{1}{2} \cdot I_6 + I_4$$

$$(19) \quad I_{12} = I_{13} = \frac{1}{2} \cdot I_6 + I_4 + I_2$$

$$(20) \quad \begin{cases} \left(R + \frac{1}{2} R_e \right) \cdot I_6 + \frac{1}{2} L_e \cdot \frac{dI_6}{dt} = \frac{1}{2} R \cdot 2I_4 \\ \frac{1}{2} R \cdot 2I_4 + \frac{1}{2} R_e \cdot (2I_4 + I_6) + \frac{1}{2} L_e \cdot \frac{d(2I_4 + I_6)}{dt} = \frac{1}{2} R \cdot 2I_2 \\ \frac{1}{2} R \cdot 2I_2 + \frac{1}{2} R_e \cdot (2I_2 + 2I_4 + I_6) + \frac{1}{2} L_e \cdot \frac{d(2I_2 + 2I_4 + I_6)}{dt} = R \cdot I_1 \end{cases}$$

$$(21) \quad \begin{cases} \left(R + \frac{1}{2} R_e \right) \cdot (1 - A - 2B - 2C) \cdot I_L + \frac{1}{2} L_e \cdot (1 - A - 2B - 2C) \cdot \frac{dI_L}{dt} = R \cdot C \cdot I_L \\ R \cdot C \cdot I_L + \frac{1}{2} R_e \cdot (1 - A - 2B) \cdot I_L + \frac{1}{2} L_e \cdot (1 - A - 2B) \cdot \frac{dI_L}{dt} = R \cdot B \cdot I_L \\ R \cdot B \cdot I_L + \frac{1}{2} R_e \cdot (1 - A) \cdot I_L + \frac{1}{2} L_e \cdot (1 - A) \cdot \frac{dI_L}{dt} = R \cdot A \cdot I_L \end{cases}$$

where: I_1, \dots, I_6 – currents flowing into grounding electrodes, I_{XY} – currents flowing between controllers CX and CY.

We have provided only input equations for calculation of factors A , B and C for Configuration 3. The analytical solution of these equations has a complicated form, so they have been solved numerically.

Assume that the lightning current I_L has the waveform of 20 kA, 2/50 μ s. These parameters are close to the average observed for natural lightning strikes [12]. Hence, in (3)-(21) current I_L equals to 20 kA and the current front steepness dI_L/dt is approximately 10 kA/ μ s (= 20 kA / 2 μ s).

Transmission-line (TL) and simple PSpice models

In order to assess the performance of the developed SC models, the results of calculation of currents flowing through the sensor cables and of potentials at the controllers'

enclosures (at the grounding electrodes as indicated in Fig. 1) are compared to the results obtained using the transmission-line (TL) model adopted from [7]-[8]. Distances between neighboring controllers are $2l = 800$ m. The TL model for Configuration 1 is shown as an example in Fig. 4.

The results of calculations have also been compared with the outputs of PSpice [9] simulations using simple circuits shown in Figs. 5 and 6. The aim of this comparison was to check if the simple lumped Π -type (Pi-type) or T-type two-ports may be used for modeling of cables. They are called the RL, RLC-Pi, and RLC-T models, respectively.

Unlike the SC models, the TL and the PSpice models apply the double-exponential approximation of the lightning current waveform [13]:

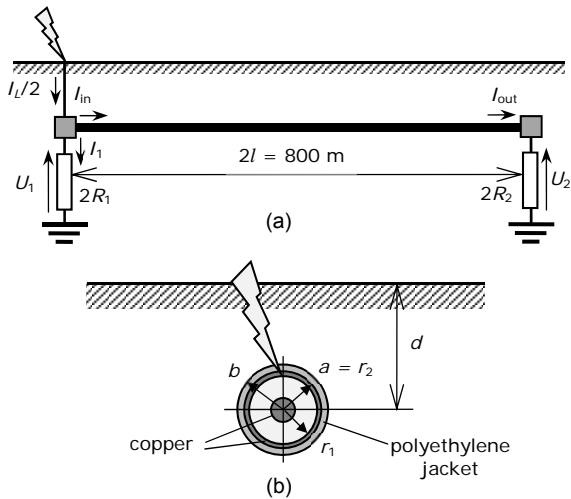


Fig. 4. Transmission-line (TL) model (a) and cross-section of single cable (b) (controllers and terminators are not modeled)

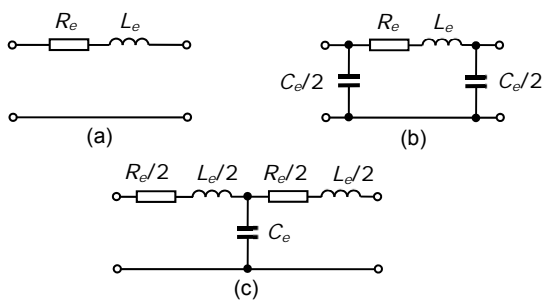


Fig. 5. Lumped PSpice models of two parallel cables of length $2l$: RL model (a), RLC-Pi model (b), RLC-T model (c)

$$(22) \quad I_L(t) = k_I I_m [\exp(-\alpha_1 t) - \exp(-\alpha_2 t)]$$

where: $k_I = 1.07$, $\alpha_1 = 1.5292 \times 10^4$, $\alpha_2 = 1.1888 \times 10^6$, $I_m = 20$ kA, t – time.

The equivalent capacitance C_e of two parallel sensor cables of length $2l$ has been calculated using formula [7]:

$$(23) \quad C_e = 4 \times \frac{2\pi\epsilon_0\epsilon_{ri}l}{\ln(b/a)}$$

where: $l = 400$ m – base length of single cable; ϵ_0 – permittivity of vacuum (F/m); $\epsilon_{ri} = 2.3$ – relative permittivity of the external insulation of the sensor cable.

Schemes created using PSpice [9] for Configuration 2 are shown in Fig. 6 as examples of modeling. Additional resistors Rx of very small resistance ($10^{-6} \Omega$ each) have been inserted to the PSpice RLC-Pi models for proper calculation of the cable input currents (Fig. 6b).

The calculations have been carried out assuming that all the grounding resistances are equal to 10Ω . According to our calculations, the grounding resistance of 10Ω corresponds to different alternative earthing terminations:

- single vertical earthing rod of 10 m in length ($\phi = 17.2$ mm), buried in soil of $100 \Omega\text{m}$ resistivity; or
- four vertical earthing rods located in corners of square 10×10 m, each of them 5 m in length ($\phi = 17.2$ mm), buried in soil of $200 \Omega\text{m}$ resistivity; or
- single horizontal earthing rod of 20 m in length ($\phi = 10$ mm), buried at 80 cm depth in soil of $100 \Omega\text{m}$ resistivity; or
- radial system of four horizontal earthing rods, each of them 10 m in length ($\phi = 10$ mm), buried at 80 cm depth in soil of $200 \Omega\text{m}$ resistivity.

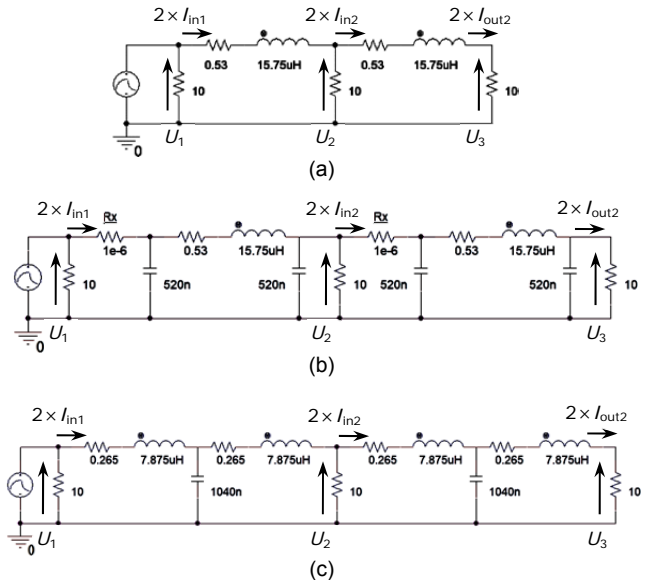


Fig. 6. PSpice schemes of Conf. 2 (Fig. 1b): RL (a), RLC-Pi with added resistors R6 and R7 (b), RLC-T (c)

Results of calculations using simple circuit (SC), transmission-line (TL) and PSpice models

Results of calculations of maximal values of currents and voltages using the models described in the previous sections are presented in Table 2.

Table 2. Results of calculations (peak values)

Conf.	Current or voltage	TL model	SC model	PSpice model		
				RL	RLC-Pi	RLC-T
1	I_{in1} (kA)	2.93	3.5	4.81	7.35	8.15
	I_{out1} (kA)	3.38	3.5	4.81	4.62	4.22
	U_1 (kV)	141.4	129.6	116.7	92.0	86.7
	U_2 (kV)	67.7	70.4	96.2	92.3	84.3
2	I_{in1} (kA)	2.93	4.0	6.15	7.35	8.15
	I_{in2} (kA)	1.23	1.4	2.98	4.87	6.0
	I_{out2} (kA)	1.35	1.4	2.98	3.30	3.09
	U_1 (kV)	141.4	119.6	113.4	76.7	75.3
3	U_2 (kV)	52.7	52.1	65.1	56.3	53.7
	U_3 (kV)	27.0	28.3	59.7	66.0	61.7
	I_{in1} (kA)	2.27	2.9	3.93	4.17	4.48
	I_{in2} (kA)	0.978	1.12	2.25	3.24	3.62
	I_{in3} (kA)	0.323	0.29	0.74	2.13	2.53
	I_{out3} (kA)	0.329	0.29	0.74	0.88	0.82
	U_1 (kV)	109.3	84.2	83.4	46.0	50.8
	U_2 (kV)	40.9	35.5	39.7	31.8	26.4
U_4 (kV)	16.3	16.6	30.3	26.9	26.5	
	U_6 (kV)	13.2	11.6	29.4	35.1	32.6

The calculation results obtained using the SC and the PSpice models are referred to those produced by the TL model. The relative differences have been calculated as:

$$(24) \quad \text{relative diff.} = \frac{(\text{any model} - \text{TL})}{\text{TL}} \times 100\%$$

where: any model – result of calculations using the SC or PSpice model; TL – output of the TL model.

Relative differences (24) are shown in Table 3.

Both the SC and PSpice models overestimate the currents and underestimate the potentials at the elements near the point of lightning strike. The more complex is the sensor configuration, the larger are the relative differences with respect to the TL model. These observations indicate that the relative differences are mainly due to the travelling wave phenomenon (Figs. 7a and 8a), which is not taken into account in the SC and PSpice models.

Surprisingly, the outputs of SC model are definitely closer to the results of TL model than PSpice ones (Tables

2 and 3). Some of the PSpice simulation results show underestimation of about 50 % or overestimation up to about 700 % with respect to the TL model. The largest underestimation produced by the SC model is of 23 %, which was obtained for Configuration 3. The largest overestimation of SC model is of 36.5 % for Configuration 2.

Table 3. Results – relative differences referred to TL model (24)

Conf.	Current or voltage	SC model (%)	PSpice model		
			RL (%)	RLC-Pi (%)	RLC-T (%)
1	I_{in1}	+19.5	+64.2	+151	+178
	I_{out1}	+3.6	+42.3	+36.7	+24.9
	U_1	-8.3	+17.5	-34.9	-38.7
	U_2	+4	+42.1	+36.3	+24.5
	Relative diff. (%)	-8.3 / +19.5	+17.5 / +64.2	-34.9 / +151	-38.7 / +178
2	I_{in1}	+36.5	+110	+151	+178
	I_{in2}	+13.8	+142	+296	+388
	I_{out2}	+3.7	+121	+144	+129
	U_1	-15.4	-19.8	-45.8	-46.7
	U_2	-1.1	+23.5	+6.8	+1.9
	U_3	+4.8	+121	+144	+129
	Relative diff. (%)	-15.4 / +36.5	-19.8 / +142	-45.8 / +296	-46.7 / +388
3	I_{in1}	+27.8	+73.1	+83.7	+97.4
	I_{in2}	+14.5	+130	+231	+270
	I_{in3}	-10.2	+129	+559	+683
	I_{out3}	-11.9	+125	+167	+149
	U_1	-23	-23.7	-57.9	-53.5
	U_2	-13.2	-2.9	-22.2	-35.4
	U_4	+1.8	+85.9	+65	+62.6
	U_6	-12.1	+123	+166	+147
	Relative diff. (%)	-23 / +27.8	-23.7 / +130	-57.9 / +559	-53.5 / +683
Maximum relative difference (%)	-23 / +36.5	-23.7 / +142	-57.9 / +559	-53.5 / +683	

The waveforms generated by the PSpice models considerably differ from those produced by the TL model. Examples of calculated waveforms are shown in Figs. 7-8. They illustrate large discrepancies between the TL model and the models called here the PSpice models. It should be noted that the “PSpice models” is the term used in this paper only, so the above statements do not mean any disadvantage of the PSpice code. It is obvious that consistency with the results of TL model can be better using RLC circuits that are more complex than those presented in Fig. 5. However, this paper is aimed at searching for a very simple model dedicated for engineering estimation of maximum values of lightning-caused overvoltages. The SC model shows up to be useful for such purposes since the observed relative differences (24) are acceptable.

More advanced approximation, using a source of surge current in connection with simple lumped-element circuits, may turn out to be useless, as in this paper. Therefore only outputs of the TL and SC models are analyzed further.

Obviously, despite the differences in results, the highest threat is observed to the system components located close to the point of lightning strike. These elements are subject to substantial threat of:

- electrical breakdown at the interfaces of the equipment (potential of order of over 100 kV referred to the remote ground);
- surge current thermal effects (currents through the sensor cables around 3-4 kA).

Components located further are subject to considerably lower stress. The electrical withstand of the polyethylene insulation of the thickness typical to sensor cables [11] is estimated to about 100 kV. However, the withstand of the electronic components is much lower than this value.

The results shown in Table 2 for Conf. 1 and 2 indicate that expansion of the open system by additional sensors may slightly increase the lightning threat at the equipment interfaces. This is because higher currents flow through the sensor cables to the grounding electrodes of the additional controllers. On the other hand, overvoltages in the loop configuration (Conf. 3) are slightly lower than those in the other configurations since the current has two parallel paths through the cables in the loop. Note that this does not mean that the loop is generally less threatened than the other configurations since its collection area [1] can be larger.

The results obtained using the SC model with different simplification regarding the sensor cable equivalent inductance was presented in [10]. However, due to a mistake in calculations for Conf. 3, those results were valid only for Conf. 1 and 2.

Analysis of grounding conditions using SC models

Assume that all the grounding resistances in the studied configurations shown in Fig. 1 are the same and equal to R . Resistance R is subject to change from 1 Ω to 10 Ω . A study of changes of maximum values of currents and voltages using only the SC models has been carried out. The results of the analysis are presented in Figs. 9-10.

Both currents and voltages change several times while changing the grounding resistances in the analyzed range.

The results show that the currents flowing through the sensor cables located close to the point of lightning strike are strongly dependent on the grounding resistance, particularly in its lower range of 1-4 Ω .

The impact of the grounding resistance on the voltages (potentials of grounding electrodes) is even stronger, particularly on those controllers that are located farther from the point of lightning strike.

Conclusion

The comparison of the proposed simple circuit (SC) model with the transmission-line (TL) model and simplified circuits applying the PSpice simulation revealed significant differences between the results. Both the SC and PSpice models show overestimation of the currents flowing in the sensor cables and underestimation of the potentials at the grounding electrodes located close to the point of lightning strike. These differences can be explained mainly by neglecting the distributed nature of RLC parameters of the cables, the skin effect and the travelling wave phenomenon. These are taken into account only in the TL model.

The results obtained using the SC model for all the studied configurations are definitely much closer to outputs of TL model than the results of simulations applying PSpice. This indicates that the SC model may be applied when rough engineering estimation of lightning threat is required.

It should be noted that the term “PSpice model” is used here only as a conceptual shortcut, which shows using PSpice for the circuit modeling with the double-exponential sources. Disadvantages of those models are related to their simplicity, not to the features of the PSpice code.

The strongest stress related to lightning current injection is observed at the components of the system located close to the point of strike. These elements are subject to high threat of electrical breakdown at the equipment interfaces and of surge current thermal effects. The exposure of the elements farthest away from the impact point cannot be neglected either. Surge protective devices should be installed at both ends of the cables in all the studied cases.

Reduction of grounding resistances is important for the performance of lightning protection measures. This results in reduction of overvoltages that is particularly efficient in the low range of analyzed grounding resistance, below 4 Ω .

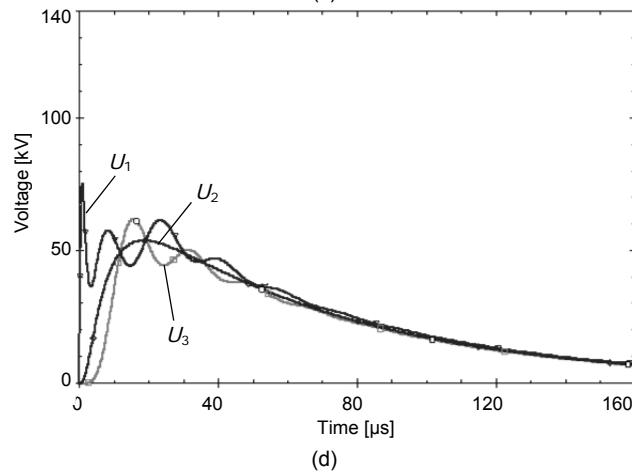
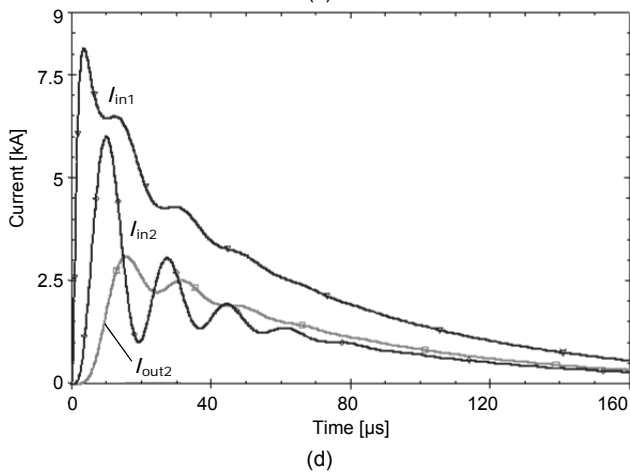
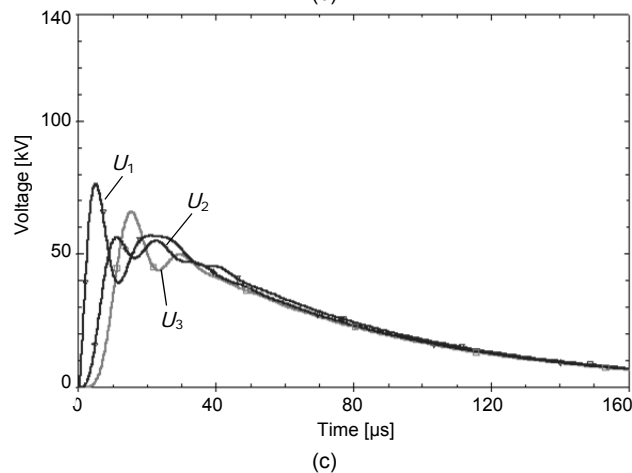
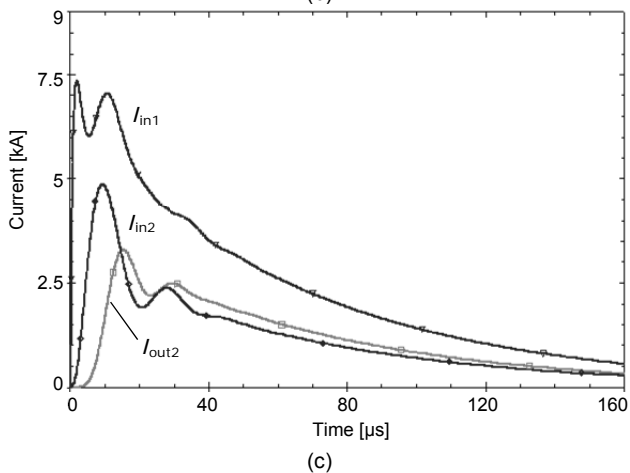
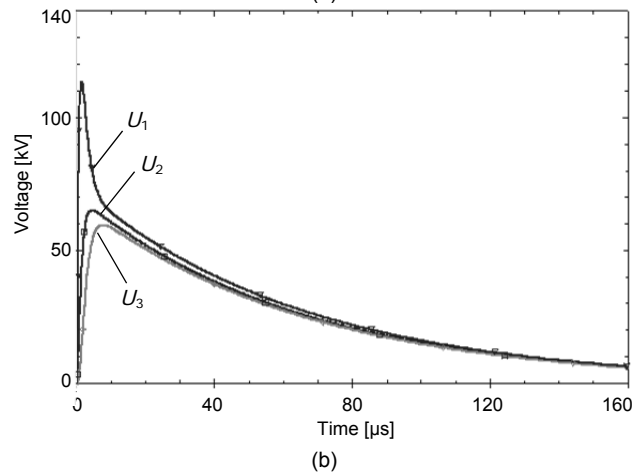
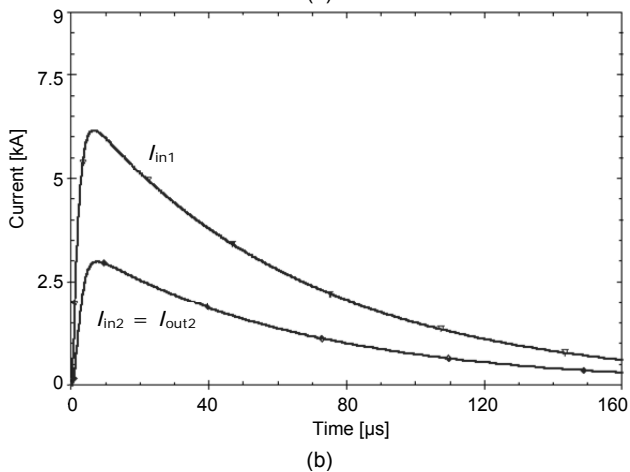
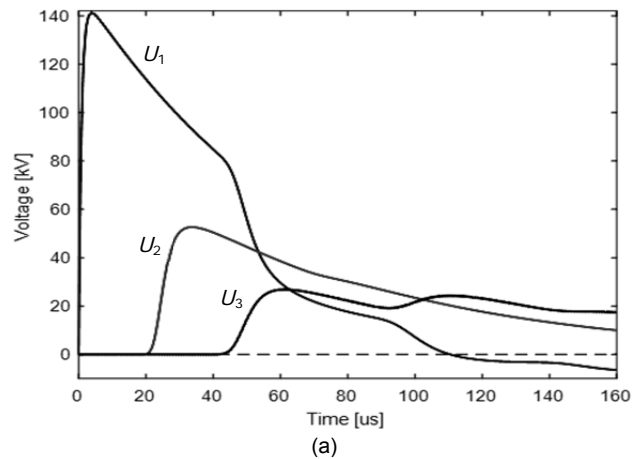
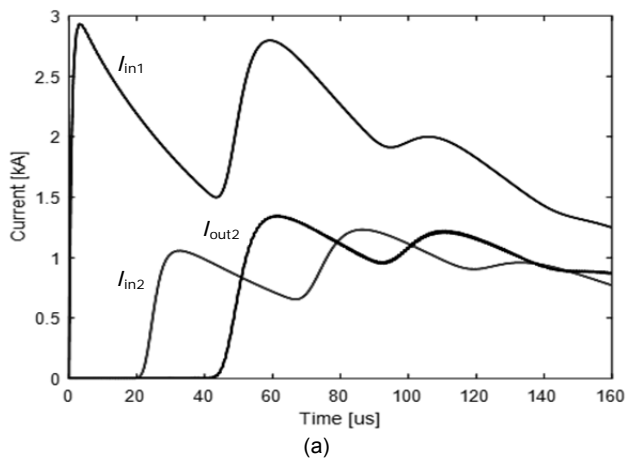


Fig. 7. Surge currents calculated for Conf. 2 using the following models: TL (a), RL (b), RLC-Pi (c), and RLC-T (d)

Fig. 8. Surge voltages calculated for Conf. 2 using the following models: TL (a), RL (b), RLC-Pi (c), and RLC-T (d)

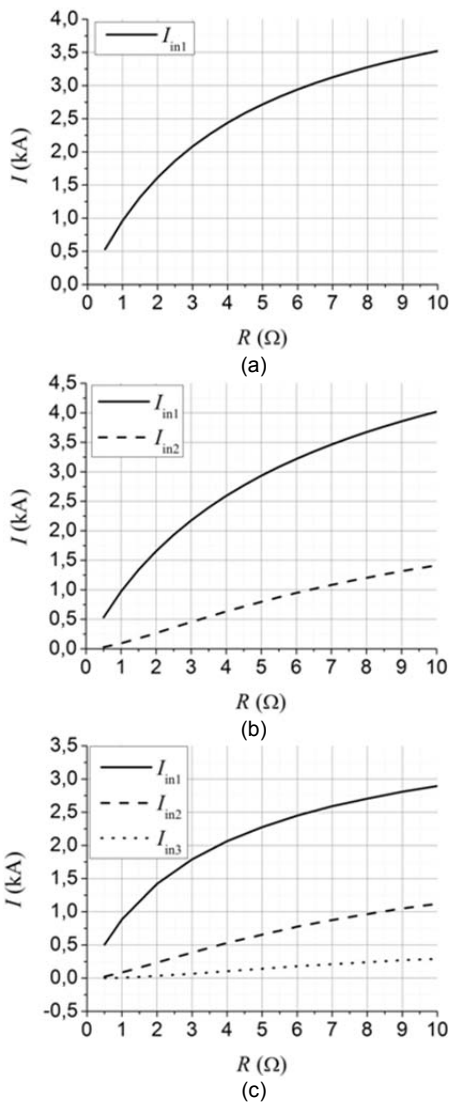


Fig. 9. Maximum values of currents calculated for Conf. 1 (a), Conf. 2 (b), and Conf. 3 (c)

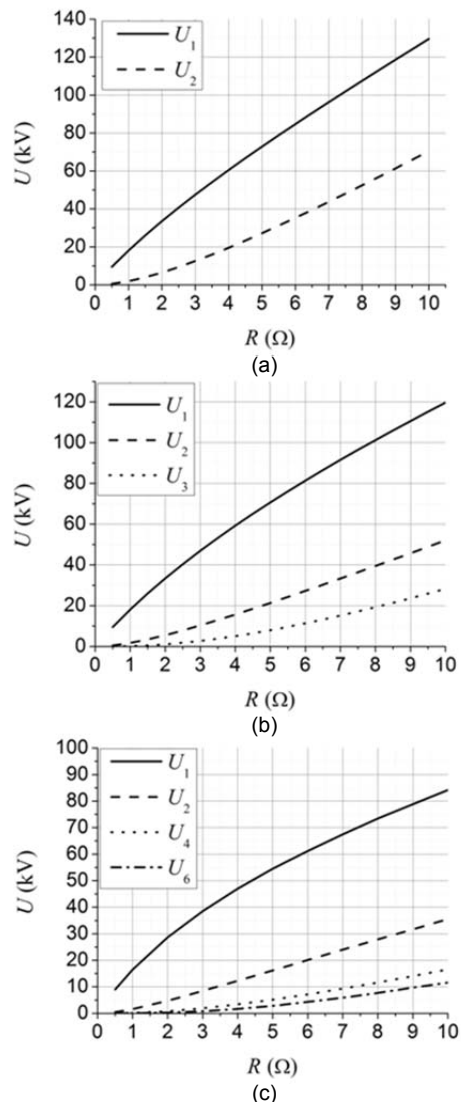


Fig. 10. Maximum values of voltages calculated for Conf. 1 (a), Conf. 2 (b), and Conf. 3 (c)

Acknowledgment: The research was conducted within the project S/W/E/1/2015, financially supported by Polish Ministry of Science and Higher Education.

Authors: dr hab. inż. Renata Markowska, Politechnika Białostocka, Wydział Elektryczny, ul. Wiejska 45d, 15-351 Białystok, E-mail: r.markowska@pb.edu.pl; dr hab. inż. Karol Aniserowicz, prof. nzw. w PB, Politechnika Białostocka, Wydział Elektryczny, ul. Wiejska 45d, 15-351 Białystok, E-mail: k.aniserowicz@pb.edu.pl.

REFERENCES

- [1] IEC 62305-1/-3, Protection against lightning, Part 1: General principles, Part 3: Physical damage to structures and life hazard
- [2] Sowa A., Ochrona urządzeń oraz systemów elektronicznych przed narażeniami piorunowymi, OWPB, Białystok 2011
- [3] Doziemny system ochrony obwodowej HF400R, STEKOP S.A. (Catalog card, in Polish, www.stekop.pl)
- [4] Barbosa C. F., Zeddani A., Day P., Bourgeois Y., Effect of guard wire in protection a telecommunication buried cables struck by rocket-triggered lightning, *Proc. of 29th International Conference on Lightning Protection*, 23-26 June 2008, Uppsala, Sweden, p. 6b-1-1–6b-1-6
- [5] Ziemia R., Maślowski G., Kossowski T., Analysis of the overvoltages caused by nearby lightning stroke, *Proc. of 24th International Conference on Electromagnetic Disturbances EMD'2017*, 20-22 September 2017, Białystok, Poland, 147-150
- [6] Alipio R., Segantini R. C., Electromagnetic disturbances propagation along a grounding grid subjected to lightning currents, *Proc. of 24th International Conference on Electromagnetic Disturbances EMD'2017*, 20-22 September 2017, Białystok, Poland, 1-4
- [7] Vance E. F., Coupling to shielded cables, Wiley – Interscience, 1978
- [8] Aniserowicz K., Markowska R., Semi-analytic calculations of overvoltages caused by direct lightning strike in buried coaxial cable, *Proc. of XXIV International Conference on Electromagnetic Disturbances EMD'2017*, 20-22 September 2017, Białystok, Poland, 9-12
- [9] OrCAD PSpice Designer v. 17.2 Lite, OrCAD Cadence PCB Solutions, 2016
- [10] Markowska R., Aniserowicz K., Exposure of underground cable intrusion detection system to overvoltages caused by lightning strike, *Proc. of 24th International Conference on Electromagnetic Disturbances EMD'2017*, 20-22 September 2017, Białystok, Poland, 73-76
- [11] Technical data sheet – *Radiating cables*, Kabelwerk, EUPEN AG, Rev.: 08/2010-10-07
- [12] Uman M. A., Natural lightning, *IEEE Trans. on Industry Applications*, vol. 30, no. 3, May/June 1994, 785-790
- [13] Aniserowicz K., Analysis of electromagnetic compatibility problems in extensive objects under lightning threat (monograph, pdf available at <http://pbc.biaman.pl/dlibra>, in Polish), Białystok 2005